Chemical Colloids versus Biological Colloids: A Comparative Study for the Elucidation of the Mechanism of Protein Fiber Formation†

Shaohua Xu,*,‡,§ David Wu,§ Morton Arnsdorf,§ Robert Johnson,|| Godfrey S. Getz,⊥ and Veneracion G. Cabana⊥

Florida Space Research Institute, Space Life Sciences Laboratory, Kennedy Space Center, Florida 32899, Department of Medicine and Pathology, The University of Chicago, Chicago, Illinois 60637, and Abbott Laboratory, Abbott Park, Illinois 60064

Received December 2, 2004

ABSTRACT: Fiber formation from murine serum amyloid A1 (SAA) was compared to the linear aggregation and fiber formation of colloidal gold particles. Here we report the similarities of these processes. Upon incubation with acetic acid, SAA misfolds and adopts a new conformation, which we termed saa. saa apparently is less soluble than SAA in aqueous solution; it aggregates and forms nucleation units and then fibers. The fibers appear as a string of the nucleation units. Additionally, an external electric field promotes saa fiber formation. These properties of saa are reminiscent of colloidal gold formation from gold ions and one-dimensional aggregation of the gold colloids. Colloidal gold particles were also found to be capable of aggregating one-dimensionally under an electric field or in the presence of polylysine. These gold fibers resembled in structure that of saa fibers. In summary, protein aggregation and formation of fibers appear to follow the generalized principles derived in colloidal science for the aggregation of atoms and molecules, including polymers such as polypeptides. The analysis of colloidal gold formation and of one-dimensional aggregation provides a simple model system for the elucidation of some aspects of protein fiber formation.

Proteins exhibit some of the physical−chemical properties of colloids. Colloidal particle formation and aggregation represent an energy minimization process. This has been well studied. Physical laws have been derived over the last two centuries for the formation and aggregation of colloids. The question is, then, whether these physical laws can be applied to protein aggregation, particularly that of the amyloidogenic proteins. Deposition of protein fibers in vivo is believed to be responsible for a class of heterogeneous diseases, including Alzheimer's disease, prions, mad cow disease, and systemic amyloidosis. The last of these examples is sometimes associated with the overexpression of the serum amyloid A protein that occurs in certain chronic inflammatory diseases.

The process of amyloidogenesis is often the result of incorrect folding or reduced hydrophilicity of partially proteolyzed molecules present at relatively high levels, possibly as a result of increased expression or decreased degradation. Additionally, this could arise because of amino acid mutations in proteins, whose wild type is fully soluble. These molecules are thought to have greatly reduced solubility compared to their precursors and exist in vivo in a supersaturated state. The supersaturated solution provides an environment that is optimal for aggregation and amyloid fiber formation. Perturbations that promote amyloid fiber formation in vitro have been extensively investigated, including seeding (*1*, *2*), agitation, aging, and hemodialysis (*3*). Despite this, the pathway for the amyloid fiber formation has not been fully characterized. Although there is no sequence homology among amyloidogenic proteins, there may still exist commonalities in their pathways to amyloid deposits. The properties observed for amyloid protein aggregation resemble the formation and aggregation of colloidal particles.

Formation and aggregation of chemical colloids are well understood. "Colloid", derived from the Greek word "glue", is used to describe those particles that are suspended in a medium of a different phase, for example, clouds, smog, ink, and milk (*6*−*8*); they diffuse slowly, in contrast to crystalline compounds (*9*). Biomacromolecules all fall into the category of solid colloidal suspensions in an aqueous medium, as originally characterized by Thomas Graham in 1862 (*9*). The large surface areas of colloidal particles allow the adsorption of ions from the bulk solution and the consequent generation of an electrochemical potential on the colloids. This potential is particularly important for the stability of the colloids; a reduction of this potential would lead to colloidal aggregation.

In our previous publications, we reported the one-dimensional aggregation of an amyloidogenic yeast protein, Sup35, and a nonamyloidogenic human plasma protein, low-density lipoprotein. We compared their aggregation to

† This work was supported in part by a development grant from the Department of Medicine, The University of Chicago, by the University of Chicago−Argonne National Laboratory Collaborative Grant Programs (to S.X.), by R44GM/HL56056 (M. Griem, Principal Investigator, subcontract to M.A. and S.X.), and by AHA Grant 0050505N (to V.G.C.).

* To whom correspondence should be addressed at the Florida Space Research Institute, Space Life Science Laboratory, Kennedy Space Center. Phone: 321-861-2899. E-mail: shaohua@fsri.org.

‡ Kennedy Space Center.

§ Department of Medicine, The University of Chicago.

|| Abbott Laboratory.

⊥ Department of Pathology, The University of Chicago.

10.1021/bi0474719 CCC: $30.25
Published on Web 03/12/2005

colloidal particle formation and aggregation. In the case of Sup35, we proposed a two-step model (*4*). Step 1 involves the spherical aggregation of a few dozen misfolded monomeric proteins. Hydrophobic forces drive this step and determine the shape of the aggregates to be spherical. These aggregates are named nucleation units, following the terminology used in colloidal chemistry. Step 2 involves the one-dimensional aggregation of these nucleation units driven by their intrinsic dipole moments. In the case of low-density lipoprotein, we reported that this nonamyloidogenic protein can also form one-dimensional aggregates upon perturbation and that the aggregation process appears to resemble the aggregation of chemical colloids and amyloidogenic proteins (*5*).

Particle aggregation generally involves these same two steps: formation of nucleation units and aggregation of the nucleation units (*10*). The hydrophobic force, which is directionless, drives the particles to aggregate spherically and form nucleation units. Adsorption of ions from bulk solution leads to the generation of a surface chemical potential around the nucleation units, and the potential makes the colloids repel each other. Under conditions favoring aggregation, colloids often form fractals. But, when the electrochemical forces play a significant role in the aggregation process, one-dimensional aggregates or fibers are formed (*8*). Thus, common properties, rather than common structure, lead to the formation and aggregation of chemical colloids. Amyloidogenic peptides share the property of fiber formation and Congo red adsorption to the fibers. Congo red is a dye that has been used over the last two centuries by merchants for coloring cotton (cellulose fiber), cloth, and fabrics (such as polyester of nylon) (*11*). A center question is whether amyloid fiber formation is a generic phenomenon of protein chemistry (*12*). In this paper, serum amyloid A (SAA)[1] is used to elucidate whether its fiber formation also resembles one-dimensional colloidal aggregation.

An acute-phase reactant, SAA is a 12 kDa polypeptide produced predominantly in the liver in response to inflammatory cytokines (*13*). Its plasma concentration increases more than 1000-fold within 24−48 h after an infection or a tissue-destructive process. The biological function of SAA and the significance of the massive increase in SAA concentration during an acute-phase reaction remain unclear. SAA is the precursor of the amyloid A proteins (AAs) deposited in reactive or secondary amyloidosis. The precise mechanism involved in the conversion of SAA to AA is still not clearly understood. AA can be deposited in the kidney, spleen, heart, and liver (*14*). Increased production and decreased or incomplete degradation of SAA may cause AA amyloidosis. Incubation of SAA in acetic acid results in the molecule's misfolding and the formation of a new conformer named saa, whose properties have little relation to its precursor.

In this study, we investigated whether saa fiber formation is analogous to chemical colloid formation and aggregation. In particular, we examined three hypotheses: (1) Similar to the chemical conversion of the hydrophilic gold ions to hydrophobic gold atoms, the conversion of SAA to the misfolded conformer saa results in a reduction of their solubility. This solubility drop initiates the aggregation and formation of gold and saa nucleation units, a process driven by the hydrophobic forces. (2) Both gold and saa fiber formation results from one-dimensional aggregation of the nucleation units. (3) Distinct from colloidal gold fiber formation, an asymmetric charge distribution and the associated dipole moment of the saa nucleates are responsible for their spontaneous one-dimensional aggregation.

MATERIALS AND METHODS

Mass Spectrometry. Linear matrix-assisted laser desorption/ionization (MALDI) mass spectra were recorded on a PerSeptive Biosystems (Framingham, MA) Voyager-DE PRO biospectrometry workstation. This system was equipped with a 337 nm, 3 ns pulse nitrogen laser. For protein analysis, the procedure followed was as described previously (*15*). Typically, 100 laser shots were averaged for each spectrum. Samples were dialyzed for 30−60 min by disk dialysis. One microliter of protein solution and 1 μL of matrix were deposited on the MALDI target and allowed to air-dry. The matrix consisted of a saturated solution of 3,5-dimethoxy-4-hydroxycinnamic acid (Aldrich) in an 80:20 mixture of acetonitrile−water.

Atomic Force Microscopy (AFM) Imaging. A NanoScope III AFM-1 was used as previously described (*16*). The instrument is routinely calibrated with mica to ensure accurate movement in the $x-y$ plane. The details of the tip selection and calibration procedure have also been described previously (*16*). The raw data are plane-fit, and imaged molecule dimensions were measured with the NanoScope III off-line data analysis package. Additionally, the cantilever tip sectional radius was subtracted from the apparent sectional radius of the specimen to yield the actual size.

Production of Recombinant Murine SAA. Recombinant murine SAA was produced as a fusion protein with glutathione *S*-transferase (GST) in the vector. The cDNA was produced by polymerase chain reaction; we used as a template RNA isolated from apoA-I$^{-/-}$ mouse liver 24 h after the injection of LPS. The mRNA was isolated by guanidine thiocyanate/cesium chloride as outlined previously (*17*). Oligonucleotides (Integrated DNA Technologies, Ames, IA) were prepared to contain an *Xba*I and a *Sal*I site at the 5′ and 3′ ends of the murine *Saa1* gene (5′ACGTCTAGAGGGTTTTTTTCATTTATTGGG3′ and 5′ATCGTCGACCTGAGGACCCCAACACAGCCT3′, the underlined nucleotides corresponding to Gly+1 in the first oligo and the stop codon in the second oligo). Sequencing confirmed the integrity of the *Saa1* transcript. The cDNA was subcloned into a pGEX-KG vector, transformed into bacteria, and grown, and the protein expression was induced by isopropyl thio-β-D-galactoside (*18*). Cell lysates were prepared by sonication and were incubated with glutathione−Sepharose beads (Pharmacia) for isolation of the fusion protein (GST-SAA1). After thorough washing of the glutathione−Sepharose beads with PBS (140 mM NaCl, 2.7 mM KCl,

[1] Abbreviations: AA, amyloid A; AFM, atomic force microscopy; C_{SAT}, saturation concentration for SAA; C_{NUC}, nucleation concentration for SAA; C_{SAA}, SAA concentration; C_{saa}, saa concentration; C_{nuc}, nucleation concentration for saa; C_{sat}, saturation concentration for saa; DOPG, 1,2-dioleoyl-L-α-phosphatidyl-DL-glycerol; DVM, digital video microscopy; EDTA, ethylenediaminetetraacetic acid; GST, glutathione *S*-transferase; LDL, low-density lipoprotein; LPS, lysophosphatidylserine; MALDI MS, linear matrix-assisted laser desorption/ionization mass spectrometry; MWCO, molecular weight cutoff; SAA, serum amyloid A (native); saa, serum amyloid A (misfolded).

10 mM Na_2HPO_4, 1.8 mM KH_2PO_4, pH 7.3), the SAA was cleaved from the fusion protein with thrombin (50 IU/mL bead volume) while remaining attached to the beads, yielding a highly concentrated solution of lipid-free SAA.

Preparation of Gold Particles. Colloidal gold particles (2 μL, 1.5×10^{12} particles/mL, stored in water with 0.1% NaN_3) were purchased from Sigma (St. Louis, MO) and were diluted in Millipore-filtered water (18 μL), spread onto a freshly peeled mica surface, air-dried, and stored in a desiccator at room temperature overnight.

Fiber Preparation. SAA (0.65 mg/mL in 150 mM NaCl, 10 mM sodium phosphate buffer, pH 7.0) was incubated in acetic acid overnight under ambient conditions (final acetic acid concentration, 10%). The protein solution was then diluted into an equal volume of 10% NH_3H_2O solution before being imaged with AFM. To study the effect of an electric field on fiber formation, we applied an external electric field of 1 V/cm to colloidal gold and saa solutions for 10 min. To study the effect of the dielectric constant of a solvent on fiber formation, we incubated colloidal gold particles dissolved in an 80% ethanol solution for 5 min. Specimens were then analyzed with AFM. The samples were compared to those not subject to electric field or organic solvent perturbations.

Specimen Preparation for AFM Imaging in Air and in Solution. An aliquot of protein sufficient to form a layer on mica (1 cm in diameter) was mixed into phosphate solution preloaded on mica (10 mM sodium phosphate, 100 mM NaCl, pH 7.0). The specimen was incubated at room temperature for 5 min for adsorption of the protein to the surface of the mica. For imaging in solution, the specimen was then directly mounted on the sample stage and imaged. For imaging dry, the mica disk was soaked in a weighing boat (3 cm in diameter) filled with 5 mL of phosphate solution for removal of unbound proteins, rinsed with 5 drops of water, and air-dried for at least 3 h before imaging.

Electrophoresis. Dialysis tubes (MWCO 12000−14000 Spectra/Por 2; Spectrum Laboratory Inc., Rancho Domingue, CA) were cleaned in a bath of 1 mM ethylenediaminetetraacetic acid (EDTA) and 2% w/v $NaHCO_3$ (Sigma) for 20 min. They were then flushed with distilled water. Colloidal gold (0.3 mL) and 0.7 mL of water were placed inside the dialysis tubing. New, freshly cleaned tubing was always used. The tubing now roughly 2 cm in length was placed in a 20 cm long electrophoresis box (BioMax MP1015; Kodak) filled with water or buffer solution (33 mM Na_2HPO_4, 1% EDTA, 1% NaN_3). The container was connected to a constant-current DC power source (E-C Apparatus Corp., St. Petersburg, FL); a voltage of 120 V was applied. Dialysis tubes were removed from the bath after a predetermined time, and the contents were removed via syringe extraction before visible spectroscopy analysis on a Beckman DU 640 spectrophotometer (Beckman Coulter, Inc., Fullerton, CA) or digital video microscopy (DVM) analysis.

Digital video microscopy (DVM) can resolve motionless particles as small as 200 nm and moving particles as small as 60 nm (*19*). The resolution improves if the particles naturally fluoresce, such as lipoproteins (*20*), or are adept at absorbing light, such as gold colloids. A line of ultraviolet epoxy (Norland Productions, Inc.) was drawn in a square around a 2×2 cm^2 area on top of a glass slide. Specimens were composed of 40 μL of 20 nm undiluted gold colloids mixed with 10 μL of either NaCl or poly(L-lysine) (Sigma). The samples were vigorously shaken, and 15 μL aliquots were then placed in the center of the epoxy square. A thin glass coverslip was then placed on top of the specimen just before exposure of the coverslips to UV light to cure the glue. The specimen was protected from UV light by a piece of aluminum foil placed on top of the upper coverslip above the sample. A chamber 2−3 cm long, 2 cm wide, and 100−200 μm deep was formed between the coverslip and the slide and the epoxy glue.

The sample sealed under the glass coverslip was mounted onto a slide holder. Two drops of mineral oil was spread on top of the coverslip. The sample was then placed on the specimen stage under an Olympus BH2 optical microscope with an oil immersion objective (100×, NA = 1.40). A laser beam was used for positioning the sample in the *z* direction and was turned off once the microscope was focused inside the chamber. The specimen stage was then moved manually in the *x* and *y* directions until an area of interest appeared on the TV monitor. The analogue video signal taken by a charge-coupled device video camera (Hitachi, Tokyo, Japan) mounted on the microscope was then digitized with a real-time frame grabber (LG-3) installed in a Macintosh computer (Apple, Cupertino, CA). Unless specified, data were usually taken in a window of observation of 54×40 μm^2. The observation depth was always 0.5 μm for all images.

Spectrophotometry. Gold colloid in water was mixed with pyridine (50 mM) or poly(L-lysine) (0.2 μg) in a cuvette; a 400−800 nm scan was then taken of the sample every 2 min until changes in the spectrum were no longer apparent.

RESULTS

In this report, we found that saa aggregation and formation of amyloid fibers appear to follow the colloidal theory: molecules and atoms aggregate and form colloids or nucleation units which in turn aggregate and form fractals. Specifically, we compared the aggregation of saa and colloidal gold particles, the intermediates generated, the structure of the fibers formed, and the effect of an electric field on the process. We found three similarities between the two: (1) aggregation and formation of spherical nucleation units; (2) linear assembly of the nucleation units and formation of fibers with an appearance of beaded chains; (3) the promotion of fiber formation by an electric field. These support the analogy we proposed earlier that protein aggregation and formation of fibers follow the generalized principles derived in colloidal science for the aggregation of atoms and molecules, including polymers where proteins belong to.

Colloidal Gold Fiber and saa Amyloid Fiber: Similar Morphological Appearance and Common Pathway of Formation? The saa fibers prepared by overnight incubation of SAA in 10% acetic acid were deposited on mica, rinsed with water, and imaged with AFM in air. Under AFM, two groups of spheres were identified, and they differed in size. The mean heights of the small and large beads were 7.0 ± 1.8 nm ($n = 34$) and 24.1 ± 2.2 nm ($n = 34$), respectively. The large beads are considered as the nucleation units (Figure 1, panel A) because the fibers appear as one-dimensional

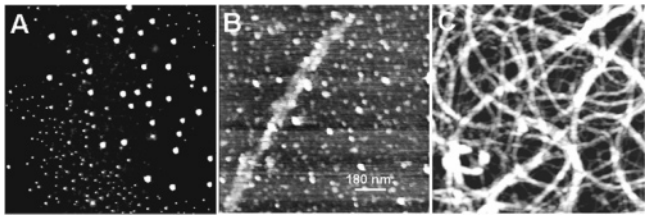

FIGURE 1: Electric field promotes saa fiber formation (AFM images). The saa fibers were prepared by incubation of SAA (0.5 mg/mL 10 mM sodium phosphate, pH 7.2) in 10% acetic acid at room temperature overnight. The mixture was then neutralized with NH_4OH solution and diluted in water. An aliquot of 50 μL of the diluted protein was applied to mica. The mica was rinsed with water after a 5 min incubation at room temperature and air-dried overnight. (A) Small and large beads. (B) Large beads and two fibers twisted together. (C) The specimen after exposure to an electric field. A multitude of fibers were found concentrated in a single area, with diminished numbers of beads elsewhere. The fibers appear as strings of large beads. (The scale bar is 180 nm for all panels.)

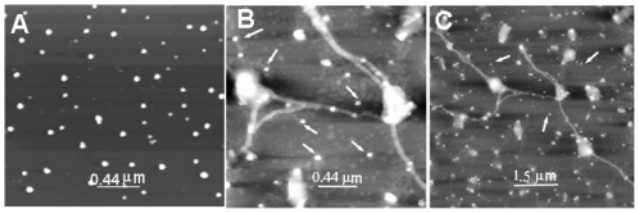

FIGURE 2: An electric field promotes gold fiber formation, as it does for the saa fibers. (A) Colloidal gold particles (diameter 10 nm) appear as spheres. (B, C) When an electric field is applied to the gold particles in solution, fibers are induced. Some gold particles remain free, as indicated by arrows. The width of the fibers is less than that of the colloidal particles.

aggregation of the large spheres (Figure 1, panel B). The small beads could be precursors of the nucleation units because they are too large to be monomeric molecules with a molecular mass of 12 kDa. The fibers shown in panel B appear to be two fibers twisted around one another. When an electric field was applied to saa, all the beads, large or small, virtually disappeared. Instead, the mica surface imaged was full of fibers (Figure 1, panel C), which suggests that the small and large beads were incorporated into the fibers.

Gold colloids can aggregate linearly under an electric field, and the fibers formed appear to be similar to those of saa fibers. Colloidal gold particles appeared as individual spheres under AFM (Figure 2A). When an electric field was applied to colloidal gold particles incubated on a mica surface, they aggregated and formed fibers (Figure 2B,C). The width of the gold fibers was less than the diameter of the colloidal gold particles. The height of these fibers was 5.3 ± 0.8 nm ($n = 20$), which is 42% lower than the height of the gold particles that did not participate in fiber formation (9.2 ± 1.0 nm, $n = 20$), suggesting continuous structural changes as the colloidal gold particles assembled into fibers. The blobs of irregular structure present in Figure 2B,C may be a result of nonlinear aggregation.

The Nucleation Unit Represents an Intermediate in saa Aggregation. Most monomeric saa molecules disappeared and were in aggregated form after 24 h of incubation in acetic acid. Aggregation of saa was analyzed by MALDI MS. Incubation of SAA with acetic acid (10%, v/v) converts highly soluble SAA to insoluble saa. The decreased solubility of saa leads to saa aggregation, as indicated by the reduction

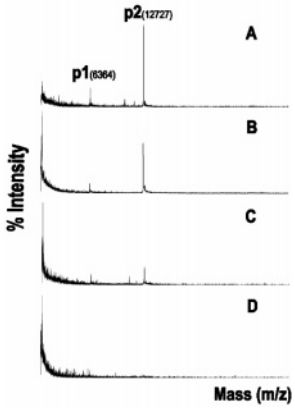

FIGURE 3: MALDI MS of saa aggregation. (A) SAA before incubation in acetic acid, (B) SAA/saa after incubation in 10% acetic acid for 60 min, (C) after 120 min of incubation, and (D) after 24 h of incubation. Peak 2 corresponds to SAA/saa with a molecular mass of 12.7 kDa. As the acetic acid incubation time increases, the amount of SAA/saa decreases, presumably due to aggregation.

of monomeric SAA/saa with incubation time (Figure 3). Although the relative intensity of the SAA/saa peak may vary for each measurement depending upon the specific area of the gold matrix analyzed, a representative group of data was acquired.

When native saa was analyzed, a major peak of 12727 Da was identified with a relative intensity of 100% (Figure 3). Since the molecular mass of saa is 12.7 kDa, peak 2 was thus assumed to be the saa peak. A second peak of less strength at 6364 Da (peak 1) was also present with a relative intensity of 25%. This corresponds to the saa that are di-ionized (traveling about half of 12727 Da). After 1 h of acetic acid incubation, peak 2 was reduced to 60% and peak 1 to 25%. After 2 h of acetic acid incubation, peak 2 was reduced to 20% and peak 1 to 15%. Both peaks 1 and 2 became insignificant after overnight acetic acid incubation, suggesting that most of the saa molecules were now aggregated.

Results from AFM images and MS spectra indicated that the nucleation units were intermediates of fiber formation. AFM images showed that the spherical intermediates were still present 24 h after the initiation of fiber formation, but those spheres were not monomeric saa; otherwise, MS would have detected their presence. The monomeric saa would appear much smaller than these large spheres shown in the AFM images.

Hydrophobic Interaction Might Be Responsible for the Aggregation and Formation of Spherical Nucleation Units. Langmuir-trough experiments (Figure 4) showed that SAA is capable of insertion into a membrane monolayer formed on an air−aqueous buffer interface, indicating that a hydrophobic region of SAA was exposed to the aqueous environment. This suggests a shortage of polar and charged residues to pack all of the nonpolar residues inside the protein core and away from the aqueous solution (*23*−*27*).

When tested with lipid, the addition of SAA to the subphase leads to an increase in the monolayer area. The area per SAA molecule inserted into the monolayer can be estimated. The monolayer was formed by addition of an aliquot of 50 μL of 1,2-dioleoyl-L-α-phosphatidyl-DL-glycerol (sodium salt) (DOPG) (0.2 mg/mL, MW 797), which corresponds to a total of 7.5×10^{15} molecules. Assuming that all proteins in the trough are bound to the membrane,

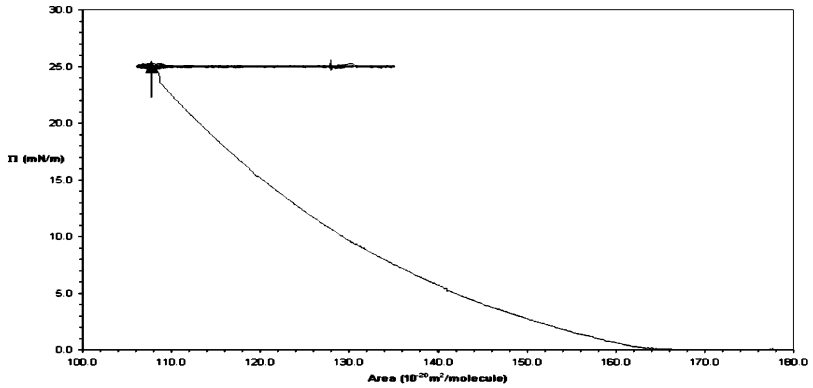

FIGURE 4: Langmuir trough experiments show that SAA has hydrophobic regions exposed to the aqueous solution that are available for membrane insertion. A monolayer of DOPG is formed in the air−buffer interface (10 mM sodium phosphate, 150 mM NaCl, pH 7.0). The density of the lipids at the air−buffer interface was controlled by the surface pressure, 25 mN/m at 30 °C. SAA was then injected into the subphase with a syringe (30 μg) (arrow). Insertion of SAA into the monolayer leads to an increase in the monolayer area.

because each DOPG molecule, at a constant membrane pressure of 25 mN/m, occupies 106 Å^2, the addition of SAA peptides (10 μg, or 6.2×10^{14} molecules) results in an increase in the total monolayer area of 23 Å^2/mol $\times$ 7.5×10^{15} molecules $= 1.73 \times 10^{17}$ Å^2. This means that each SAA peptide can increase the monolayer by 1.73×10^{17} Å^2/(6.2×10^{14} molecules) $= 2.8 \times 10^2$ Å^2/molecule. This would be equivalent to an insertion of 85 (CH_2) groups or the side chains of 17 isoleucine residues into the monolayer, suggesting that portions of the SAA surface are apolar. These calculations are unsubstantiated by two events. First, not all protein molecules may be incorporated into the interface. Second, some of the interfacial insertion may be attributable to unfolding, with exposure of additional hydrophobic residues upon the initial binding to the air−water lipid monolayer (*23*−*27*).

An increased exposure of the hydrophobic region to the aqueous environment might have triggered the aggregation process. It is anticipated that acid denaturation exposes more hydrophobic regions of the molecule. A generally observed phenomenon is that, as the proteins change from their water-soluble conformer to the less soluble and amyloidogenic conformer, there is an increase in β-sheeted structure. The globular structure allows the packing of a maximum volume of hydrophobic core by a fixed number of charged and polar residues. It would take more polar and charged residues to wrap a sheeted structure than a globular one. The increased exposure of hydrophobic regions to the aqueous environment promotes aggregation of these molecules, an energy minimization process.

Dipole Moment May Contribute to the Linear Assembly of the Nucleation Units. An electric field of 6 V/cm was sufficient to cause significant aggregation of the colloidal gold particles sealed in a dialysis bag. A change of the light spectrophotometry spectrum was detected for the gold solution. As the electrophoresis time was increased, the dominant 520 nm peak steadily fell and a peak near 700 nm steadily rose (Figure 5I). After 30 min of electrophoresis, all of the gold particles appeared to be aggregated or precipitated out of solution, as indicated by the disappearance of all major adsorption peaks and the resemblance of the spectrum to that for pure water. DVM images also revealed colloidal gold aggregates induced by electrophoresis, and the aggregates appeared to be similar to those shown in Figure 5I, D−F.

Compared to fractal formation, one-dimensional aggregation is rather exceptional for chemical colloids. A small intrinsic dipole moment in the nucleation unit may be responsible for the mostly linear aggregation of amyloidogenic proteins. However, different mechanisms might be involved in one-dimensional aggregation of saa or gold colloids induced by an electric field. An electric field might generate a concentration gradient of the protein or gold colloids. A high monomer concentration in a focal area promotes aggregation. This is because the aggregation rate is a function of the monomer concentration. Also, the presence of an external electric field induces the polarization of the surface chemical potential of the saa and gold colloids and thus dipole formation. Dipole−dipole interaction leads to aggregation of the nucleation units (*21*). After a fiber is formed, the electric field can polarize the fiber, make the fiber more attractive to incoming nucleation units through electrostatic force, and thus promote fiber growth.

Polylysine induces colloidal gold fiber formation. In the absence of any perturbations, gold colloids (diameter 20 nm) were too small to be detected by DVM, and the solution appeared clear (Figure 5IV, A). When incubated with a high concentration of poly(l-lysine), the gold colloids aggregated and produced large spheres (Figure 5IV, B,C). However, an incubation of the gold colloids with a low concentration of poly(l-lysine) resulted in gold fiber formation. The gold particles also aggregated first spherically and then linearly. These aggregates were often shorter but wider than those induced by electrophoresis of gold colloids on a mica surface but retained the appearance of a one-dimensional aggregation of the nucleation units. Up to 5 μm long gold fibers could be induced by incubation of the gold colloids with a low concentration of polylysine. Large spheres were also present. These spheres were larger than the original colloidal gold particles but similar in size to those nucleation units in the fibers and are thus considered to be nucleation units as well. The aggregated gold tended to be deposited on the lower glass coverslip, possibly due to the gravity force. This gravity force may have played a role in limiting the length of the fibers formed as well. Compared to the incubation with a high concentration of polylysine, gold colloids incubated with a low concentration of polylysine may have a better chance to form nucleation units with an uneven distribution of the charged polylysine on the gold surface. Such an uneven distribution would lead to the

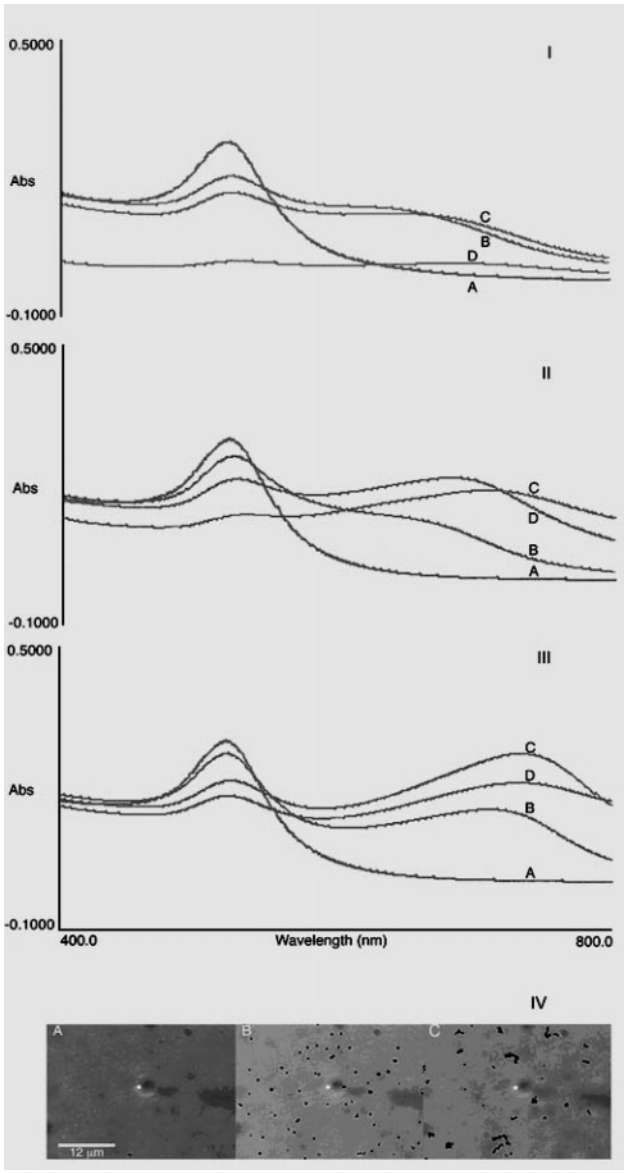

FIGURE 5: Chemical and physical perturbations on colloidal gold aggregation. (I) A sample of a 0.3 mL colloidal gold and 0.7 mL H_2O mixture underwent electrophoresis in dialysis tubing at 120 V/20 cm for varying times. (A) At time zero, the spectrum was a typical gold colloid spectrum. (B) At 5 min, the major peak has decreased, and a second peak has increased. (C) At 10 min, the whole spectrum decreased in absorbance but was very similar to that of 5 min. (D) At 30 min, the sample exhibits a spectrum similar to that of water. (II) Polylysine induces colloidal gold aggregation. (A) The colloidal gold solution. (B) 2 min after addition of 0.2 μg of poly(L-lysine), the first peak decreases and a second peak appears which is due to the aggregation of colloidal gold particles. (C) After 18 min, the second peak reaches a peak. (D) After 173 min, both peaks decrease, likely due to the precipitation of aggregates from solution. (III) Pyridine induces colloidal gold aggregation. (A) The colloidal gold solution. (B) 2 min after addition of pyridine (50 mM, final concentration), the first peak decreases and a second peak rose. The second peak is due to the adsorption of the aggregates. (C) After 20 min, the second peak reaches its maximum. (D) After 190 min, both peaks decrease, likely due to the precipitation of aggregates from solution. (IV) Polylysine induces colloidal gold aggregation as observed under digital video microscopy. Lower concentrations of poly(L-lysine) promote gold fiber formation, whereas higher concentrations promote spherical aggregation. (A) No poly(L-lysine) added. (B) 10 μL of 0.01% poly(L-lysine) added to gold colloid solution induces the formation of spherical precipitates. (C) 10 μL of 0.001% poly(L-lysine) to gold colloid solution promotes the formation of fibers of colloidal gold.

formation of permanent dipoles and their one-dimensional aggregation.

Results from spectroscopic studies also indicated that polylysine induces the aggregation of gold colloids. The 520 nm peak for the monomeric gold colloids (characteristic red color) disappeared, whereas a 750 nm peak (purplish color) rose (Figure 5II). Such phenomena were also observed for incubation with pyridine (Figure 5III) and NaCl solution (data not shown). The spectrum for gold incubated in pyridine showed a more pronounced aggregation peak than the same peak observed for polylysine or NaCl incubation, which suggests variation in the aggregation state and structure of the gold colloids for different perturbations. All adsorption peaks eventually disappeared, likely due to the precipitation of gold aggregates from the solution. An overnight incubation often yields a gold solution with an adsorption spectrum similar to that for pure water, which indicates precipitation of the gold aggregates (data not shown).

The promotion of fiber formation by chemicals could be attributed to their effect on the reduction of the surface chemical potential of the protein, the gold colloid, and the preformed fibers in solution. Aggregation of gold colloids by an increase in salt concentration can be explained as a screening effect on the repelling force originating from the surface chemical potential of the colloids (*21*). Polylysine binds to colloidal gold particles through electrostatic force and changes the surface chemical potential. When an excess amount of polylysine is present, the surfaces of the gold colloids are covered with polylysine. When the available polylysine is limited, the surfaces of the gold colloids are partially covered with polylysine, and dipoles are then formed. These dipoles chain together and form gold fibers. Blatchford et al. (*22*) have demonstrated the aggregation of colloidal gold particles via pyridine. Adsorption of pyridine lowers the surface chemical potential of the colloidal particles, decreases the repelling force between them, and thus promotes their aggregation (Figure 5III). A nucleation unit would preferably be bound to the end of a fiber where the electrostatic repulsion force is lower than that along the side wall of a fiber.

DISCUSSION

Fiber formation by saa appears to follow the colloidal theory: molecules and atoms aggregate and form colloids or nucleation units. Linear assembly of the nucleation units leads to the formation of fibers with an appearance of beaded chains. Formation of colloidal gold fibers and saa fibers is promoted by an electric field.

Formation of saa fibers was found to be a two-step aggregation process. Intermediates for the saa fiber formation were visualized with AFM and were found to include small and large beads. The small beads appear to fuse together and form large beads, or what we have termed nucleation units, which, in turn, chain together into linear fibers. Three pieces of evidence suggest that these small and large beads are intermediates in fiber formation; first, small and large beads disappear and saa amyloid fibers accumulate under an electric field; second, MS spectroscopy shows that saa monomers are absent while large beads are detected by AFM from samples 24 h after initiation of fiber formation. This two-step process and the appearance of the fibers resemble

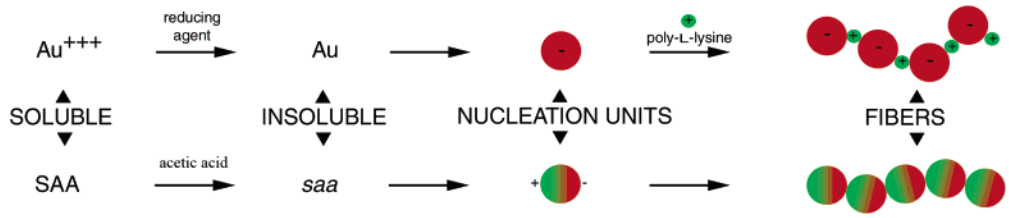

FIGURE 6: Parallel comparison of the aggregation process by chemical colloids and by biological colloids. The initial hydrophilic component undergoes transformation to become hydrophobic. Aggregating, these hydrophobic components create "nucleation units". These nucleation units assemble to form fibers if permanent dipoles are present in these nucleation units. The dipole moment could exist because of an asymmetric charge distribution or due to an uneven adsorption of charged molecules in the case of the colloidal gold particles.

the formation and the one-dimensional aggregation of colloidal particles.

Colloidal gold particles can aggregate one-dimensionally and form fibers. An electric field promotes both saa and colloidal gold fiber formation. Gold and saa fibers appear to be similar to each other as well as to Sup35 amyloid fibers (*4*). Chemicals such as NaCl, pyridine, and polylysine can also induce colloidal gold aggregation and fiber formation. Gold fibers induced by these chemicals appear to be wider compared to those induced by an electric field.

The results presented in this paper support a two-step model we introduced previously for protein aggregation and protein fiber formation (*4*, *5*). An increased exposure of hydrophobic regions leads to a spherical aggregation of the proteins and the formation of nucleation units. The asymmetric charge distribution of the nucleation units leads to their one-dimensional aggregation. Hydrophobic forces drive the first step and determine the shape of the aggregates to be spherical. The second step is driven by the dipole−dipole interaction among the nucleation units. This two-step model seems to apply to both Sup35 and saa, two amyloidogenic proteins, and to low-density lipoprotein, a "nonamyloidogenic" protein, as well as for colloidal gold particles, a typical chemical colloid (*4*, *5*). These results suggest that a general model adapted from the existing theories in colloidal chemistry may apply to aspects of protein aggregation.

When gold ions are reduced to gold atoms, the solubility decreases by 1 billion-fold for the gold element. When SAA is converted to saa by incubation in acetic acid, we suspect constants of saturation and nucleation for saa to be orders of magnitudes smaller than those for SAA. The difference of the saturation and nucleation concentrations between SAA and saa makes the aggregation and precipitation of saa from solution inevitable (Figures 6 and 7).

Colloid gold formation is an energy minimization process (*8*, *28*). Acetic acid is known to denature proteins. The nonnative conformer saa is presumed to be misfolded when compared to SAA, resulting in more hydrophobic regions being exposed to the aqueous environment. The hydrophobic forces drive the aggregation of saa and the formation of saa nucleates, an energetically favorable process. Unlike dipole−dipole interactions, hydrophobic interactions may not exhibit directionality, which determines the initial aggregation product to be spherical.

Assuming (1) the saturation and nucleation concentrations of native SAA to be C_{SAT} and C_{NUC} (Figure 7), (2) the SAA concentration to be C_{SAA}, (3) that a new molecule, saa, with a conformation different from that of SAA is generated upon acetic acid incubation, (4) the concentration of saa to be C_{SAA}, and (5) the saturation and nucleation concentrations for saa

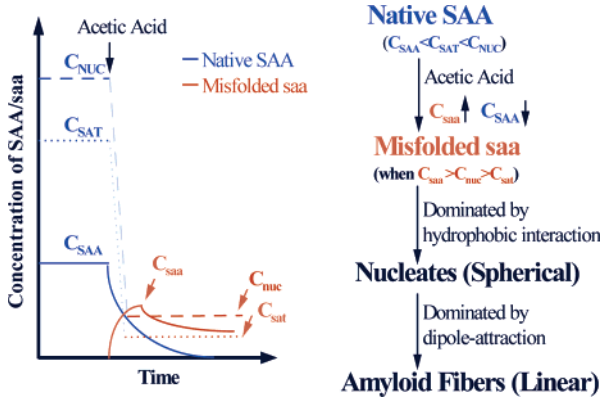

FIGURE 7: Formation of saa nucleate and fiber. Native and highly soluble SAA, when incubated in acetic acid, misfolds and forms non-native saa, a new molecule that has the same sequence as SAA but a different conformation. The constants of saturation and nucleation concentration for SAA (C_{SAT} and C_{NUC}) are much higher than those for saa (C_{sat} and C_{nuc}). SAA is stable and soluble when its concentration (C_{SAA}) is well below C_{SAT} and C_{NUC}. The acetic acid incubation results in a solution with oversaturated saa. This oversaturation triggers the aggregation of saa and the formation of saa nucleates and then amyloid fibers. Thus, as acetic acid is mixed in, the saa concentration (C_{saa}) rises initially and then decreases slowly due to saa nucleate and fiber formation.

to be C_{sat} and C_{nuc}, then, at $t = 0$, $C_{SAA} > C_{saa} = 0$, and $C_{NUC} > C_{SAT} \gg C_{SAA}$, where C_{NUC} and C_{SAT} are constants. After addition of acetic acid, C_{SAA} decreases and C_{saa} increases.

When $C_{saa} > C_{nuc} > C_{sat}$, saa nucleates are formed. The aggregation continues until $C_{saa} = C_{sat}$, where C_{nuc} and C_{sat} are constants.

If hydrophobic forces drive the initial aggregation, the introduction of other forces prohibits the unlimited spherical growth of the nucleate units. Two additional forces of opposite roles become significant as a result of the increased particle size in the nucleation process: the attractive van der Waals force and the repelling electrostatic force (*7*, *29*−*31*). A surface chemical potential is generated on the gold colloids because of adsorption of anions from bulk solution. This surface chemical potential contributes to an electrostatic repelling force between the colloids, which prevents them from further aggregating and stabilizes these particles in solution. A similar chemical potential could also be generated for the saa nucleates because of the intrinsic charges of the peptides, as well as due to ions adsorbed from bulk solution.

Further aggregation of the saa or the gold nucleates is a result of increased attractive or decreased repelling force among these colloids. A number of chemical and physical factors are known to affect colloidal stability. These factors exercise their effect by changing one or more of the following

properties: the kinetic energy (thermal or physical agitation), the surface chemical potential (surfactants, pH, solvent, salt), van der Waals force (external electric field), hydrophobic interaction (chaotropic or kosmotropic agent), and others (*10*).

The surface chemical potential of aggregated colloids is different from that of the individual colloids, and this difference is responsible for the one-dimensional aggregation and gold fiber formation. The chemical potential surrounding a spherical colloid is homogeneous in all directions. On the other hand, this potential at the end of a string of colloids would be less than that along its length, which means less repelling force on the approaching colloidal particles at the end than along the length of a fiber (*8*). Thus, it is more likely for a free colloidal particle to bind to the end of a fiber than to the length, which leads to the elongation of a fiber. Different from chemical colloids, biological colloids such as saa nucleates have an intrinsic and permanent dipole moment because of their asymmetric charge distribution. This permanent moment makes saa fiber formation kinetically more favorable than for gold. This is main test in the relative length and frequency of saa and gold colloid linear aggregation. As a result, spontaneous fiber formation is often observed for amyloid-forming proteins and peptides, whereas gold fiber formation often requires an additional reduction of the repulsive force or an increase in the attractive force, including chemical−physical perturbations. Incubation of colloidal gold with pyridine and polylysine would result in an asymmetric potential around the spheres and thus promote their linear assembly.

In a previous paper, we applied this dipole interaction model to the explanation of a number of intriguing questions about amyloid fiber formation (*4*), including the template phenomena, the seeding effect, and the absence of sequence homology among amyloid-forming fibers, as well as the diverse size distribution of the nucleation units and fibers by the same or different peptides (*32*). For example, amyloid fibers of various diameters are formed from the same molecule under various conditions. In colloidal gold chemistry, this is a well-understood phenomenon. By controlling the kinetics of the reduction reaction, one can synthesize colloidal gold particles and then gold fibers of the desired size. Thus, by controlling the kinetics of the protein misfolding and the spherical aggregation reaction, one ought to be able to control the diameter of the nucleation units and then the diameter of the fibers. Unless the surface chemical potential is much stronger along the side than at the end of a fiber, the incorporation of monomers, the nucleation units, and the association of short and thin fibers to the side wall of another should occur. The difference between the surface chemical potential along the side and at the end for short and thin fibers is not as large as for long and wide fibers (*8*). End-to-end fusion of fibers should be possible as well based on our model (*4*, *31*). Although linear aggregation is preferred, because of the aggregation kinetics, chemical colloids are capable of forming fractals; their structural features cannot be described mathematically with unitary dimensions, but only with fractional dimensions (*28*−*30*). Thus, biological colloids should be capable of one-dimensional aggregation as well as fractal formation. The branching phenomena observed for some amyloid fibers might be a simple form of fractals for amyloid fibers.

Nucleation units (the spheres) or even some soluble protein conformers are proposed in the literature to be cytotoxic, possibly by forming ion channels. Our work provides no data in this regard. However, cytotoxic channel proteins are known to kill cells with one or few molecules, such as tetanus toxin, diphtheria toxin, or colicins (*33*). Amyloidosis often is progressive and caused by accumulation of pathogenic molecules. In addition, the time of action is very different. Channel toxins usually act within hours or days, not decades. The development is often acute in toxin-induced diseases, not chronic as observed in amyloidogenic ones.

In summary, the chemical nature and the internal structure of the nucleation units are obviously different between saa and colloidal gold units, but both are products of an energy minimization process. This also explains their similarity in the production of nucleation units as well as the linear assembly and formation of fibers. Such process has now been demonstrated by six proteins, namely, saa, Sup35 (*4*), LDL (*5*), Tau40, α-syn, and A-β (unpublished data). We suspect this pathway might be shared by other proteins in formation of amyloid fibers.

ACKNOWLEDGMENT

We thank Dr. Ka Yee C. Lee for the use of the Langmuir trough and Canay Ege for showing us how to perform the trough experiments.

REFERENCES

1. Lansbury, P. T., Jr. (1997) Yeast prions: inheritance by seeded protein polymerization?, *Curr. Biol. 7*, R617−R619.
2. Uversky, V. N., and Fink, A. L. (2004) Conformational constraints for amyloid fibrillation: the importance of being unfolded, *Biochim. Biophys. Acta 1698*, 131−153.
3. Tang, S. Y., and Pepys, M. B. (1994) Amyloidosis, *Histopathology 25*, 403−414.
4. Xu, S., Bevis, B., and Arnsdorf, M. F. (2001) The assembly of amyloidogenic yeast sup35 as assessed by scanning (atomic) force microscopy: an analogy to linear colloidal aggregation?, *Biophys. J. 81*, 446−454.
5. Xu, S., and Lin, B. (2001) The mechanism of oxidation-induced low-density lipoprotein aggregation: an analogy to colloidal aggregation and beyond?, *Biophys. J. 81*, 2403−2413.
6. Hirtzel, C. S., and Rajagopalan, R. (1985) in *Colloidal Phenomena: Advanced Topics*, pp 15−23, Noyes, Park Ridge, NJ.
7. Evans, D. F., and Wenneerstrom, H. (1994) *The Colloidal Domain: Where Physics, Chemistry, Biology, and Technology Meet*, pp 187−238, VCH, Weinheim, Germany.
8. Bradley, J. S. (1994) in *Clusters and Colloids* (Schmid, G., Ed.) pp 459−536, VCH, Weinheim, Germany.
9. Fruton, J. S. (1972) in *Molecules and Life: Historical Essays on the Interplay of Chemistry and Biology*, pp 131−132, Wiley & Sons, New York.
10. Jullien, R., and Botet, R. (1987) in *Aggregates and Fractal Aggregate*, pp 77−102, World Scientific Publishing Co., Singapore.
11. Meloan, S. N., and Puchtler, H. (1978) Demonstration of amyloid with Mesitol WLS-Congo Red: application of a textile auxiliary to histochemistry, *Histochemistry 58*, 163−166.
12. Fändrich, M., Fletcher, M. A., and Dobson, C. M. (2001) Amyloid fibrils from muscle myoglobin, *Nature 410*, 165−166.
13. Ureili-Shoval, S., Linke, R. P., and Matzner, Y. (2000) Expression and function of serum amyloid A, a major acute-phase protein, in normal and disease states, *Curr. Opin. Hematol. 7*, 64−69.
14. Cabana, V. G., Lukens, J. R., Rice, K. S., Hawkins, T. J., and Getz, G. S. (1996) HDL content and composition in acute phase response in three species: triglyceride enrichment of HDL a factor in its decrease, *J. Lipid Res. 37*, 2662−2674.
15. Gorisch, H. (1988) Drop dialysis: time course of salt and protein exchange, *Anal. Biochem. 173*, 393−398.

16. Xu, S., and Arnsdorf, M. F. (1994) Calibration of the scanning (atomic) force microscope with gold particles, *J. Microsc. (Oxford) 173*, 199−210.
17. Patel, H., Bramall, J., Waters, H., deBeer, M. C., and Woo, P. (1996) Expression of recombinant human serum amyloid A in mammalian cells and demonstration of the region necessary for high-density lipoprotein binding and amyloid fibril formation by site-directed mutagenesis, *Biochem. J. 318*, 1041−1049.
18. Cabana, V. G., Reardon, C. A., Wei, B., Lukens, J. R., and Getz, G. S. (1999) SAA-only HDL formed during the acute phase response in apoA-I+/+ and apoA-I−/− mice, *J. Lipid Res. 40*, 1090−1103.
19. Crocker, J. C., and Grier, D. G. (1996) Methods of digital microscopy for colloidal studies, *J. Colloid Interface Sci. 179*, 298−310.
20. Akimova, E. I., and Melgunov, V. I. (1984) Apolipoprotein B: removal of lipids by sodium cholate and reassociation of a lipid-free apoprotein with dipalmitoyl phosphatidylcholine, *Biochem. Int. 9*, 463−473.
21. Halsey, T. C. (1993) Electrorheological fluids-structure and dynamics, *Adv. Mater. 5*, 711−718.
22. Blatchford, C. G., Campbell, J. R., and Creighton J. A. (1982) Plasma resonance−enhanced Raman scattering by absorbates on gold colloids: The effects of aggregation, *Surf. Sci. 120*, 435−455.
23. Wu, H. (1931) Studies on denaturation of proteins XIII. A theory of denaturation, *Chin. J. Physiol. 5*, 321−344 [reprinted in (1995) *Adv. Protein Chem. 46*, 6−26].
24. Honig, B. (1999) Protein folding: from the Levinthal Paradox to structure prediction, *J. Mol. Biol. 293*, 283−293.
25. Chan, H. S., and Dill, K. A. (1990) Origins of structure in globular proteins, *Proc. Natl. Acad. Sci. U.S.A. 87*, 6388−6392.
26. Kauzmann, W. (1959) Some factors in the interpretation of protein deenaturation, *Adv. Protein Chem. 14*, 1−63.
27. Kurutz, J., and Xu, S. (2001) Hofmeister solute effects on hydrophobic adhesion forces in SFM experiments, *Langmuir 17*, 7323−7326.
28. Israelachvili, J. (1994) in *Intermolecular and Surface Forces*, pp 67−82, Academic Press, San Diego, CA.
29. Winslow, W. (1949) Induced fibration of suspensions, *J. Appl. Phys. 20*, 1137−1145.
30. Witten, T. A., Jr., and Sander, L. M. (1981) Diffusion-limited aggregation, a kinetic critical phenomenon, *Phys. Rev. Lett. 47*, 1400−1403.
31. Halsey, T. C., Duplantier, B., and Honda, K. (1997) Multifractal dimensions and their fluctuations in diffusion-limited aggregation, *Phys. Rev. Lett. 78*, 1719−1722.
32. Harper, J. D., Wong, S. S., Lieber, C. M., and Lansbury, P. T. (1999) Assembly of A beta amyloid protofibrils: an in vitro model for a possible early event in Alzheimer's disease, *Biochemistry 38*, 8972−8980.
33. Xu, S., Cramer, W. A., Peterson A. P., Hermodson, M., and Montecucco, C. (1988) Dynamic properties of membrane proteins: reversible insertion into membrane vesicles of a colicin E1 channel-forming peptide, *Proc. Natl. Acad. Sci. U.S.A. 85*, 7531−7535.

BI0474719